major product[14] with a very small amount of II. After methylation of the crude material, a mixture was obtained. It was found to contain 98% of VIII and 2% of III, identical with an authentic sample (cis isomer) as it could be confirmed by VPC and ^{1}H NMR, using a *B,B′,B″*-trimethyl-*N,N′,N″*-tri-*o*-tolylborazine-enriched sample. *B,B′,B″*-Triethyl-*N,N′,N″*-tri-*o*-tolylborazine (IV) was also prepared, for the same purpose, but this compound was found more difficult to purify and the ethyl substituent attached to boron led to a complex second-order pattern (A_2B_3 in ^{1}H NMR), rendering difficult accurate identification.

Conclusion

When performed under very mild conditions (refluxing diethyl ether), the reaction of CH_3MgI with *B,B′,B″*-trichloro-*N,N′,N″*-tri-*o*-tolylborazine (1) leads to the *cis-B,B′,B″*-trimethyl-*N,N′,N″*-tri-*o*-tolylborazine as the sole isomer. The trans isomer of III could not be obtained, either in the course of the previous reaction or by heating the cis isomer above its melting point. Instead, significant amounts of *B*-hydroxy byproducts, essentially V, are produced, resulting from incomplete methylation of I: they probably originate from unreacted trans isomer of I because of steric reasons. More drastic conditions (refluxing in aromatic solvent for instance) have been used[15,16] for the reaction of Grignard compounds RMgX with such crowded *B,B′,B″*-trichloro-*N,N′,N″*-triarylborazines: in every case, the yield of *B,B′,B″*-trialkyl-*N,N′,N″*-triarylborazine was very low, probably because of extensive ring opening. Finally, the reported formation of the trans isomer in those experiments[3] seems somewhat questionable.

Acknowledgment. We are most grateful to the reviewers for a number of valuable comments and suggestions. We are much indebted to Professor J.-L. M. Abboud for helpful discussions.

Registry No. I, 5775-58-6; III, 749-85-9; IV, 52176-11-1; V, 96413-88-6; VII, 96413-89-7; VIII, 42168-28-5; BCl_3, 10294-34-5; MeI, 74-88-4; EtI, 75-03-6; BBr_3, 10294-33-4; *o*-toluidine, 95-53-4.

---

(14) S. Allaoud, M. El Mouhtadi, and B. Frange, unpublished results.

(15) C. A. Brown and A. W. Laubengayer, *J. Am. Chem. Soc.*, **77**, 3699 (1955).

(16) L. F. Hohnstedt and D. T. Haworth, *J. Am. Chem. Soc.*, **82**, 89 (1960).

Contribution from the Department of Chemistry,
Montana State University, Bozeman, Montana 59717

Reaction of Nickel(II) *N,N′*-Bis(2-aminoethyl)malonamidate(2−) with Triethylenetetramine

JON P. STORVICK and GORDON K. PAGENKOPF*

Received November 8, 1984

The reaction of triethylenetetramine with a nickel complex that has an internal six-membered chelate ring and terminal amine donors exhibits rate constants comparable to those observed for reactions with similar nickel–polypeptide complexes. The six-membered chelate ring does increase the rate constants for the reaction with H_3O^+ however. The rate constant values (25.0 °C, $I = 0.10$ M) are $k_{H_2O} = 0.001$ s^{-1}, $k_{H_3O} = 3.9 \times 10^6$ M^{-1} s^{-1}, $k_T = 0.25$ M^{-1} s^{-1}, $k_{HT} = 0.73$ M^{-1} s^{-1}, and $k_{H_3T} = 1.5 \times 10^2$ M^{-1} s^{-1}.

Introduction

The reactions of nickel(II)–short-chain polypeptide complexes with triethylenetetramine ($Trien_T$) proceed through a variety of different pathways. Complexation of nickel by triglycine[1] establishes the general basic configuration of low-spin square-planar complexes. Nickel transfer from this ligand to trien follows three general pathways: one that is trien and proton independent, one that is trien dependent, and one that is proton dependent. As portions of the peptide ligand are altered, there are dramatic changes in the competitiveness of each pathway.[2-10]

This study utilized a tetradentate ligand *N,N′*-bis(2-aminoethyl)malonamide, BAEM, which forms two five-membered chelate rings and one six-membered chelate ring with Ni(II) (I). The configuration of the six-membered chelate is critical to the kinetic stability. The transfer of Ni(II) from this complex to trien to form $Ni(trien)^{2+}$ proceeds through the three general pathways, and the rate constant values are markedly different from what has been observed for the diglycylethylenediamine complex.[10]

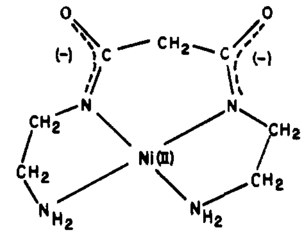

I

Experimental Section

N,N′-Bis(2-aminoethyl)malonamide, BAEM, was synthesized from diethyl malonate and ethylenediamine.[11] A 0.0991 M $Ni(ClO_4)_2$ solution was prepared from the recrystallized salt and standardized by EDTA titration. The complexes were formed by the addition of 50% excess ligand to a $Ni(ClO_4)_2$ solution. The ionic strength was maintained at 0.100 M through the addition of the appropriate amount of 2.0 M $NaClO_4$. The initially acidic solutions were slowly adjusted to the desired pH, which was 9.0 or greater, by adding NaOH. All solutions were bubbled with N_2 in an attempt to eliminate any complex oxidation. Borate buffer, $B_T = 0.005$ M, was utilized for the reactions in the pH

---

(1) Billo, E. J.; Margerum, D. W. *J. Am. Chem. Soc.* **1970**, *92*, 6811–6818.

(2) Paniago, E. B.; Margerum, D. W. *J. Am. Chem. Soc.* **1972**, *94*, 6704–6710.

(3) Billo, E. J.; Smith, G. F.; Margerum, D. W. *J. Am. Chem. Soc.* **1971**, *93*, 2635–2641.

(4) Mason, C. F. W.; Chamberlain, P. I.; Wilkins, R. G. *Inorg. Chem.* **1971**, *10*, 2345–2348.

(5) Bannister, C. E.; Margerum, D. W. *Inorg Chem.* **1981**, *20*, 3149–3155.

(6) Pagenkopf, G. K.; Brice, V. T. *Inorg. Chem.* **1975**, *14*, 3118–3119.

(7) Raycheba, J. M. T.; Margerum, D. W. *Inorg. Chem.* **1980**, *19*, 837–843.

(8) Bannister, C. E.; Raycheba, J. M. T.; Margerum, D. W. *Inorg. Chem.*, **1982**, *21*, 1106–1112.

(9) Pearson, R.; Pagenkopf, G. K. *Inorg. Chem.* **1978**, *17*, 1799–1803.

(10) Storvick, J. P.; Pagenkopf, G. K. *Inorg. Chem.* **1985**, *24*, 1827–1830.

(11) Ojima, H.; Yamada, K. *Nippon Kaguku Zasshi* **1970**, *91*, (1), 49–53.

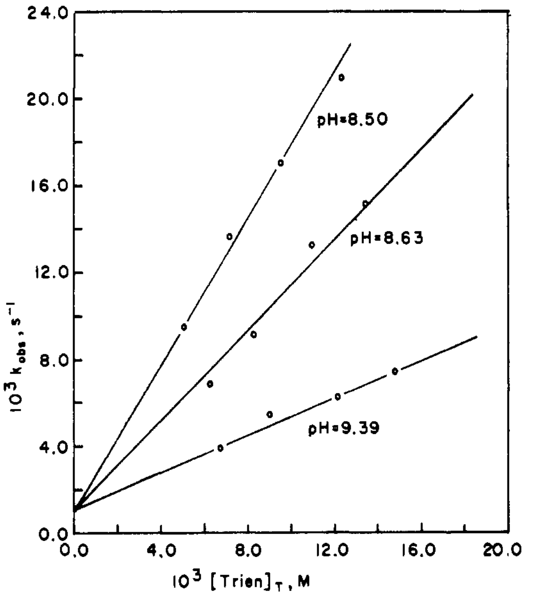

Figure 1. Dependence of k_{obsd} on the Trien$_T$ concentration in the pH 8-10 range.

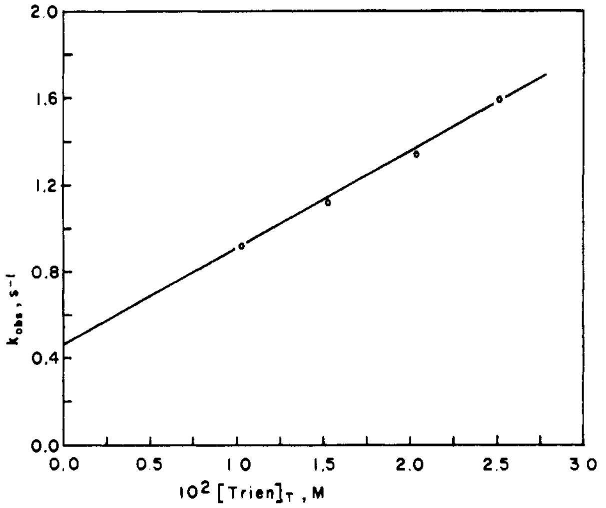

Figure 2. trien and proton dependence for the reaction of Trien$_T$ with NiH$_{-2}$BAEM at pH 7.04.

8-10 region. No buffer was used for the pH 10-11.5 range, and Trien$_T$ was used as the buffer for the pH 8 down to pH 5 range. The concentration range for the complex was (0.7-40.0) × 10^{-3} M. Trien$_T$ was always kept in excess. The absorption maximum for NiH$_{-2}$BAEM is 440 nm with a molar absorptivity of 35 M^{-1} cm^{-1}. The monitored pH values were converted to hydrogen ion concentration by the extended Debye-Hückel relationship. All reactions were run at 25.0 °C. The trien solutions were prepared through dilution of aliquots taken from a 0.100 M stock. The trien pK_a values used to resolve the rate constants are $pK_{HT} = 9.74$, $pK_{H_2T} = 9.08$, and $pK_{H_3T} = 6.56$.[12]

The reactions were followed spectrophotometically by observing a decrease in absorbance with time. The slow reactions were monitored with 10.0-cm cells and a Varian 634 spectrophotometer; the fast reactions, with a Durrum 103 stopped-flow spectrophotometer. The reactions were always run under pseudo-first-order conditions. The rate constants are the average of three runs. A nonlinear-least-squares computer program, LLJAC, was utilized to fit the data.[13]

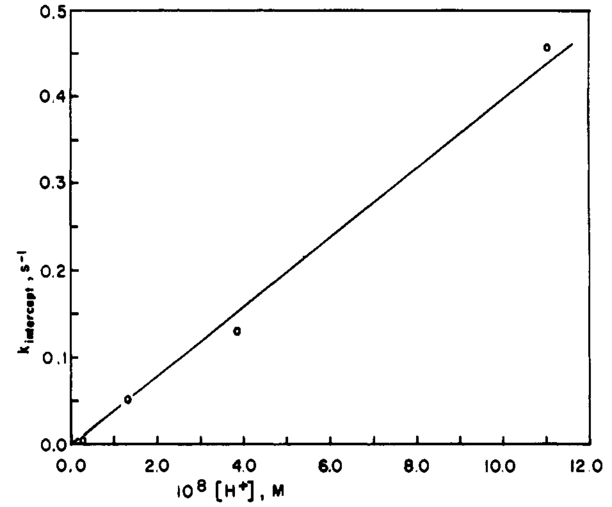

Figure 3. Dependence of the intercept constants on the hydrogen ion concentration (slope = k_{H_3O} = 3.9 × 10^6 M^{-1} s^{-1}).

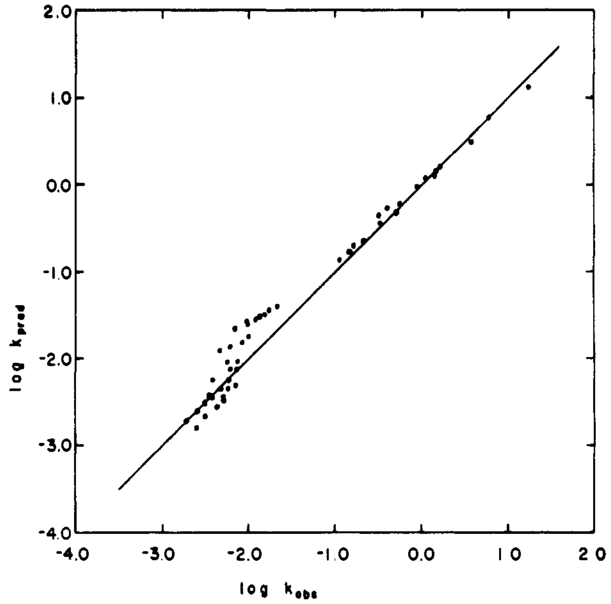

Figure 4. Agreement between the observed rate constants and the predicted rate constants.

Table I. Rate Constants for the Reaction of trien with NiH$_{-2}$MBAE

constant	value	constant	value
k_{H_2O}	(1.0 ± 0.2) × 10^{-3} s^{-1}	k_{H_3T}	(1.5 ± 0.1) × 10^2 M^{-1} s^{-1}
k_T	0.25 ± 0.06 M^{-1} s^{-1}	k_{H_3O}	(3.9 ± 0.5) × 10^6 M^{-1} s^{-1}
k_{HT}	0.73 + 0.16 M^{-1} s^{-1}		

Results

The reaction of NiH$_{-2}$BAEM with Trien$_T$, which is shown in eq 1, exhibits sizable variation with pH.

$$\text{NiH}_{-2}\text{BAEM} + \text{Trien}_T \xrightarrow{H^+} \text{Ni(trien)}^{2+} + \text{BAEM} \qquad (1)$$

The reactions were always run under pseudo-first-order conditions, which provides the relationship shown in eq 2. The rate constant k_{obsd} was

$$-d[\text{NiH}_{-2}\text{BAEM}]/dt = k_{obsd}[\text{NiH}_{-2}\text{BAEM}] \qquad (2)$$

determined from plots of ln $(A - A_\infty)$ vs. t (A is absorbance). An increase in Trien$_T$ concentration provides a linear increase in the observed rate constants, as demonstrated in Figure 1. In the highest pH range (8-11.5) the same nonzero intercept is observed, but as the pH decreases to the region of 7, the intercept shows a major increase (Figure 2). These observations lead to eq 3.

$$\text{rate} = (k_{H_2O} + k_{H_3O}[H_3O^+] + k_{TT}[\text{Trien}_T])[\text{NiH}_{-2}\text{BAEM}] \qquad (3)$$

Combination of the intercept values provides Figure 3. The value of k_{H_2O} from Figure 1 is 0.001 s^{-1}, and k_{H_3O} = 3.9 × 10^6 M^{-1} s^{-1} from Figure 3.

It is possible that all four Trien$_T$ species (T, HT^+, H_2T^{2+}, and H_3T^{3+}) could be contributing to the rate. Analysis of the data

---

[12] Smith, R. M.; Martell, A. E. "Critical Stability Constants"; Plenum Press: New York, 1975; Vol. 2.

[13] Howald, R. A. "LLJAC Program", Montana State University, 1983.

indicates, however, that the contribution from H_2T^{2+} is not competitive, and thus no k_{H_2T} rate constant can be determined. The rate expression is shown in eq 4. Rate constants for the three

$$-d[NiH_{-2}BAEM]/dt = (k_{H_2O} + k_{H_3O}[H_3O^+] + k_T[trien] + k_{HT}[Htrien^+] + k_{H_3T}[H_3trien^{3+}])[NiH_{-2}BAEM] \quad (4)$$

reactive trien species, H_2O, and H_3O^+ are listed in Table I, and the agreement between $k_{predicted}$ and k_{obsd} is shown in Figure 4. The observed rate constant range is 4 orders of magnitude.

Discussion

Proton Transfer. Complexation of nickel(II) by ligands such as triglycine (GGG), *N,N′*-bis(2-aminoethyl)oxalamide (ODEN), diglycylethylenediamine (DGEN), and diglycylhistidine (GGHis) provides planar orientation of the deprotonated, coordinated amide nitrogens. The ligand used in this study, BAEM, is similar to ODEN in that both have five membered side chelate rings with terminal amine donors. The back chelate rings differ, however, in that ODEN has a five-membered ring whereas BAEM has an added $-CH_2-$ and thus forms a six-membered chelate ring. This change appears minimal until one attempts to make molecular models. Coordination to nickel(II) in the high-pH range shows that two protons have been removed, thus indicating that coordination is similar to that exhibited by the other ligands. Preparation of molecular models does not verify this, however. In general, insertion of $-CH_2-$ in the back chelate ring causes marked orientation stress. If one of the deprotonated amide groups is maintained planar with nickel and the two terminal amines, great disorientation within the other amide group occurs and, in fact, coordination to nickel would be minimal. As a consequence, there appear to be two major reorientations of complexed $H_{-2}BAEM^{2-}$. The first and probably most important is lengthening of the nickel–imide bonds. The amount that the bonds are lengthened is balanced by an increase in the tetrahedral bond angle of the $-CH_2-$ group in the six-membered chelate ring, as shown in diagram II. The lengthening of the Ni–imide nitrogen bonds permits more planar orientation of the coordinated amide groups. There is no apparent influence on the coordination of the terminal amine groups, however.

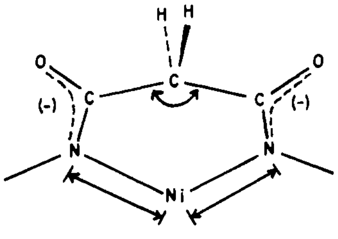

II

These two factors are indicated by the spectra of the complex. The molar absorptivity of $NiH_{-2}BAEM$ is low (35 M^{-1} cm^{-1}), and the maximum at 440 nm represents a much smaller UV shift upon deprotonation. The complex with three five-membered chelate rings, $NiH_{-2}ODEN$, has a much higher molar absorptivity (187 M^{-1} cm^{-1}) at a more energetic wavelength, 414 nm. Since the wavelength shift for $NiH_{-2}BAEM$ is not comparable to those for other nickel(II)–polypeptide complexes, it should react faster than the others, and this is observed to be the case.

For example, $NiH_{-2}BAEM$ reacts 41 times more rapidly than $NiH_{-2}GGG^-$ and 550 times more rapidly than $NiH_{-2}ODEN$. This sizable increase is primarily due to the size of the interior chelate ring. The complex formed by ODEN has a five-membered interior chelate ring. In addition, the other two chelate rings are the same as those in $NiH_{-2}BAEM$, and thus the rate constants for these provide a very direct indication of the impact. Rate constants for the other complexes are summarized in Table II.

Table II. Proton-Transfer Rate Constants for Deprotonated Nickel Complexes

complex	k_{H_3O}, M^{-1} s^{-1}	k_{H_2O}, s^{-1}	ref
$NiH_{-2}GGG$	9.5×10^4	8.6×10^{-2}	5
$NiH_{-2}DGEN$	8.5×10^3	3.0×10^{-4}	10
$NiH_{-2}ODEN$	7.0×10^3	1.0×10^{-3}	14
$NiH_{-2}ODPN$	1.2×10^5	1.0×10^{-3}	15
$NiH_{-2}GGhis$	3×10^4	8.0×10^{-5}	8
$NiH_{-2}BAEM$	3.9×10^6	1.0×10^{-3}	this work

Reaction with Trien. The reaction of trien with $NiH_{-2}BAEM$ is slower than what has been observed for the reaction with $NiH_{-2}GGG^-$, but it is similar to the rate of replacement of other ligands that have terminal amine groups, such as DGEN,[10] ODEN,[14] and ODPN.[15] The rate of dissociation of the terminal amine donors is less than what has been observed for the rate of NH_3 or $EtNH_2$[16] dissociation and thus is a reflection of the kinetic stability of the chelate rings.

In this particular case, $Htrien^+$ reacts about 3 times faster than trien. Why $Htrien^+$ reacts this much faster is not known, but it may be due to ion-pair formation. A proton-transfer pathway may be competitive, but no rate constant could be obtained for H_2trien^{2+}. This was primarily because the contributions from $Htrien^+$ and H_3trien^{3+} dominate the reactivity pattern and overshadow any H_2trien^{2+} component.

The rate constant for H_3trien^{3+} is 1.5×10^2 M^{-1} s^{-1}, which is a sizable increase over the less protonated trien ligands. This increase indicates that nickel transfer from BAEM to trien may be general-acid catalyzed or facilitated through the formation of an ion pair. Since a rate constant for H_2trien^{2+} could not be determined and no dependence upon the borate buffer concentration was observed, there is minimal evidence for a competitive general-acid-catalysis path. The k_{H_3T} constant should also be about a factor of 10 larger than the observed value. The molecular models do indicate, however, that protonation of the oxygen atoms may be more difficult than protonation of the amide nitrogens, and thus a general-acid reaction sequence could be preferred. The parallel reaction pathways are summarized in eq 5–9.

$$NiH_{-2}BAEM + H_2O \xrightarrow{k_{H_2O}} products \quad (5)$$

$$NiH_{-2}BAEM + trien \xrightarrow{k_T} products \quad (6)$$

$$NiH_{-2}BAEM + Htrien^+ \xrightarrow{k_{H_3T}} products \quad (7)$$

$$NiH_{-2}BAEM + H_3trien^{3+} \xrightarrow{k_{H_3T}} products \quad (8)$$

$$NiH_{-2}BAEM + H_3O^+ \xrightarrow{k_{H_3O}} products \quad (9)$$

The $NiH_{-2}BAEM$ reactivity pattern is unique in that the value of k_{H_3O} is the largest for a four-nitrogen-donor complex; however, the rate of BAEM replacement by trien is reduced by the presence of the terminal amines.

In summary, the expansion of the interior chelate ring from five to six members greatly facilitates the proton-transfer process. This has minimal, if any, effect upon the trien reactions, however, since the substitution sequence involves dissociation of the terminal amine groups, whose positions are not altered by expansion of the interior chelate ring.

Registry No. I, 75965-30-9; $Trien_T$, 112-24-3.

---

(14) Gilmore, K. E.; Pagenkopf, G. K., submitted for publication in *Inorg. Chem.*

(15) Gilmore, K. E. Ph.D. Thesis, Montana State University, Bozeman, MT, Aug 1984.

(16) Rorabocher, D. B.; Melendez-Cepeda, C. A. *J. Am. Chem. Soc.* **1971**, *93*, 6071–6076.